SENSOR MONITORING DRIVEN IDENTIFICATION OF HETEROGENEOUS WORKING CONDITIONS FOR MACHINE TOOL

Zhenggeng Ye[1*], Yongwei Ke [2], Xin Wang[2], Zhiqiang Cai[2]

[1]School of Management, Zhengzhou University, Zhengzhou, China.
[2]School of Mechanical Engineering, Northwestern Polytechnical University, Xi'an, China.
**yezhenggeng@zzu.edu.cn*

Keywords: SENSOR DATA; HETEROGENEOUS; CONDITIONS; IDENTIFICATION; MACHINE TOOL.

Abstract

With the development of intelligent manufacturing, real-time and adaptive RUL prediction will become a strong demand for intelligent processing centres. The heterogeneity of working conditions makes the lifetime present highly nonlinear, increasing the uncertainty of RUL prediction. Despite the development of various adaptive RUL prediction methods, the identification technique of heterogeneous working conditions is still a gap. To realize an adaptive or real-time RUL prediction, the identification of current working conditions and state transition trajectories of future working conditions is necessary. Therefore, by utilizing various monitored sensor data, a similarity evaluation method for working-condition identification is proposed. First, two features, the deviation between the probability density functions (PDF) in amplitude domain and the cross-correlation coefficient in time domain, are constructed. Then, a similarity evaluation method is proposed by constructing the similarity level of two sensor data samples, where two different evaluating indexes are provided for the similarity level. The one is evaluated by the average difference of sample features from different sensors under two different working conditions, and another is by the Euclidean distance of sample features under two different working conditions. Then, a comparison method based on 24 time-domain and frequency-domain features is given to verify the performance of the proposed method. At last, a case study based on a degradation dataset of milling insert is provided, proving the effectiveness of our proposed method. Also, the impact of different data manipulations on the accuracy rate of identifications is discussed in the case study.

1. Introduction

The degradation of the cutting tool is an important factor that affects the surface quality and dimensional accuracy of the processed workpiece [1]. In general, a premature replacement of a tool will lead to insufficient utilization of its actual life. On the contrary, the excessive utilization of a worn tool will result in tool breakage, scrapped parts, and increased downtime [2]. Therefore, it is essential to accurately predict the remaining useful lifetime (RUL) of a cutting tool [3]. However, the heterogeneity of working conditions makes RUL present highly nonlinear, increasing the uncertainty of RUL prediction.

Heterogeneity is a widespread characteristic in multifarious engineering systems [4], [5], [6]. Based on the classification in Reference [7], the heterogeneity includes the unit-to-unit variability, the variability in time-varying operating conditions, and the diversity of tasks and workloads of a system. Also, it has been indicated that RUL without considering heterogeneity will be heavily biased [8]. In current studies, many reliability or RUL analysis considers heterogeneity [9], [10], such as the dynamic linear degradation model for degradation paths that do not regularly evolve through time [11], the Wiener process model with random drift parameter for heterogeneous degradation [12], and the heterogeneity of environment in mining equipment [13], [14] and dump trucks [15].

With the development of intelligent manufacturing, real-time and adaptive RUL prediction will become a strong demand for intelligent processing centres. Considering the impact of heterogeneity in environmental or operational conditions on degradation processes, an adaptive prognostic approach was proposed for battery RUL prediction [16]. Considering the few-shot character of fault diagnosis of real, an adaptive knowledge transfer by continual weighted updating of filter Kernels was proposed to improve the fault diagnosis of machines [17]. Despite the development of various adaptive fault prognosis and RUL prediction methods, the identification technique of heterogeneous working conditions is still a gap. To realize an adaptive or real-time fault prognosis and RUL prediction, the identification of current working conditions and state transition trajectories of future working conditions is necessary.

Recognizing the above-discussed gap, the goal of this study is to explore an effective method for identifications of heterogeneous working conditions, to further fill in the blanks in real-time or adaptive fault prognosis and RUL prediction. In detail, the characters of sensor data under heterogeneous working conditions are analyzed. Then, the features of sensor data samples are constructed in both amplitude and time domains, and a method for similarity evaluation is proposed where different evaluation indexes are provided. Further, the identification method of heterogeneous

working conditions is proposed, and a method for selecting optimal sensor combinations is provided. Besides, a comparison method is given to verify the performance of our proposed method.

At last, a degradation dataset of milling insert in a machining centre from NASA Ames Prognostics Data Repository is used to validate the effectiveness of the proposed models, where 6 sensors were used to measure the status of the machine tool. The result implies that identification performance for combined conditions is inferior to the one for individual working-condition variables. Also, it proves that the applications of original full data in four stages and normalized amplitudes could help improve the identification performance. And completeness level of sensor data in all stages has a strong relationship with the accuracy rate of identifications.

The rest of this paper is organized as follows. Section 2 proposed the detailed identification method and provides the comparison method. Section 3 gives a detailed case study and analysis of identification results. Section 4 concludes this article.

2. Methodology

2.1 Sensor data under heterogeneous conditions

In engineering practices, a wide variety of sensors are utilized to monitor the status of concerned objects, such as, current sensor, vibration sensor, and acoustic emission sensor. Assume that there exist n sensors utilized to monitor a concerned object at each interval Δt, and the sample length is l. Then, the monitored sensor data sample set at time t is denoted as,

$$\boldsymbol{D}'(t) = [\boldsymbol{d}_1'(t), \boldsymbol{d}_2'(t), ..., \boldsymbol{d}_n'(t)] = \begin{bmatrix} d_1'(1) & d_2'(1) & ... & d_n'(1) \\ d_1'(2) & d_2'(2) & ... & d_n'(2) \\ ... & ... & \ddots & ... \\ d_1'(l) & d_2'(l) & ... & d_n'(l) \end{bmatrix}, \quad (1)$$

where $\boldsymbol{d}_i'(t) = [d_i'(1); d_i'(2); \ldots; d_i'(l)]$ is the sensor data sample of the sensor i at time t (i=1,2, 3…, n) and $d_i'(j)$ is the jth sample value. As shown in Fig. 1, they are two sensor data samples obtained by a current sensor equipped at the spindle of a machining centre. The x-axis represents the sample data length, and the y-axis represents the sample values. The sample length l=9000 which could cover the single pass of the cutting tool, which includes four stages: idling, engaging, steadily cutting, and retracting.

For the operation of a machine, the working condition is time-varying. Simultaneously, corresponding sensor data will also change with the working condition. As shown in Fig. 1, there show two sensor data samples under two working conditions: the first one is monitored with the depth of cut *DOC*=1.5*mm* and *Feed*=0.50*r*/*s* at the time *t*=15*min*, and the second one is monitored with *DOC*=0.75*mm* and *Feed*=0.25*r*/*s* also at the time *t*=15*min*. The two sensor data samples are different. Therefore, the types of working conditions can be identified based on the similarity between sensor data sampled at different moments.

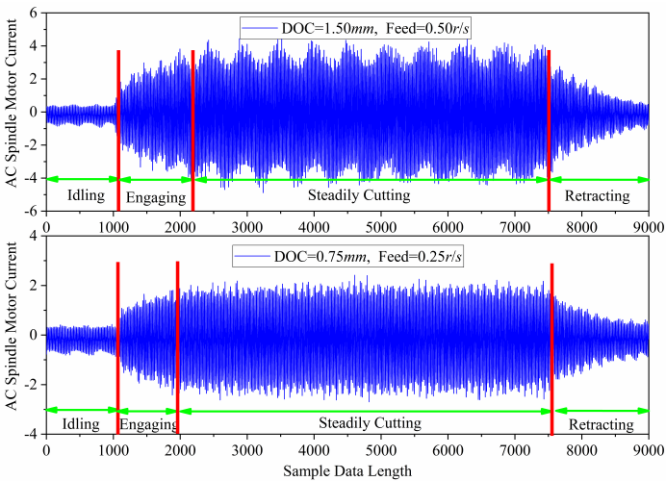

Fig. 1 Sensor data samples under different working conditions

Besides, for one given working condition, the data under different stages also show heterogeneity, as shown in Fig. 1. In the idling stage, the cutting tool does not begin cutting operating, so the sample values are steady and low. In the engaging stage, the cutting tool begins to cut the workpiece. Therefore, the sample values rise gradually. In the steadily cutting stage, the sample values are also steady but relatively high. At last, in the retracting stage, the cutting tool begins to leave the workpiece. Therefore, the sample values decrease gradually. Among data samples in different stages, the one in the steadily cutting stage is the best one reflecting the working conditions. Therefore, a comparison is studied for samples with full data in four stages and partial data in steadily cutting stages.

2.2 Feature evaluation

Before feature evaluation, the sensor data sample are normalized by the following Eq. (2),

$$\boldsymbol{d}_i(t) = \boldsymbol{d}_i'(t) / \max(\boldsymbol{d}_i'(t)), \quad (2)$$

so that the normalized sample set is

$$\boldsymbol{D}(t) = [\boldsymbol{d}_1(t), \boldsymbol{d}_2(t), ..., \boldsymbol{d}_n(t)]. \quad (3)$$

Then, for two sensor data samples $\boldsymbol{D}_1(t_1)$ and $\boldsymbol{D}_2(t_2)$, features of amplitude, time, and frequency domains are evaluated based on the normalized sensor data.

2.2.1 Amplitude Domain Feature:

In the amplitude domain, the deviation of amplitude distributions is defined as the difference between the probability density functions (PDF) of the evaluated two sensor data samples, as shown in Eq. (4).

$$D_A = \int_{-1}^{1} | f_1(x) - f_2(x) | dx, \quad (4)$$

where $f_1(x)$ and $f_2(x)$ are amplitude PDFs of the two data samples $\boldsymbol{d}_{i1}(t)$ and $\boldsymbol{d}_{i2}(t)$ obtained by the sensor i, and x is the normalized amplitude. Also, the deviation D_A can be considered as the areas between the two PDFs, as shown in Fig. 2.

Due to the normalized amplitude $x \in [-1, 1]$, we have the deviation $D_A \in [0, 2]$. Therefore, a normalized deviation degree is used as the amplitude feature of two sensor data samples, as shown in Eq. (5).

$$\hat{D}_A = \frac{1}{2} D_A . \tag{5}$$

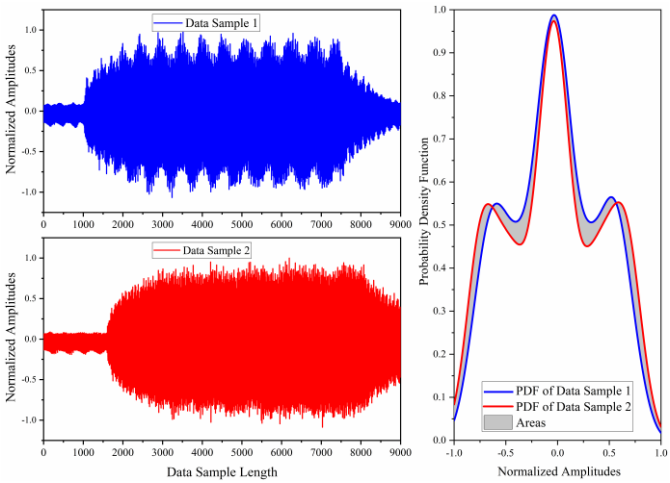

Fig. 2 Difference between PDFs

2.2.2 Time Domain Feature:

In the time domain, the cross-correlation coefficient can measure the mutual similarity between two time series, as shown in Eq. (6),

$$R_{12}(\tau) = \lim_{T\to\infty} \frac{1}{2T} \int_{-T}^{T} \boldsymbol{d}_{i1}(t)\boldsymbol{d}_{i2}(t+\tau)dt , \tag{6}$$

where $\boldsymbol{d}_{i1}(t)$ and $\boldsymbol{d}_{i2}(t)$ are data samples obtained by the sensor i, denoted as time series 1 and 2; $\boldsymbol{d}_{i2}(t+\tau)$ is the τ delay time series of the time series 2. And the normalized cross-correlation coefficient is

$$\hat{R}_{12}(\tau) = \frac{1}{\sqrt{R_{11}(0)R_{22}(0)}} R_{12}(\tau) , \tag{7}$$

where $R_{11}(0)$ and $R_{22}(0)$ are self-correlation coefficients of sensor data samples 1 and 2. Here, the maximum normalized correlation coefficient $\hat{R}_{12}(\tau)$, denoted as $\hat{R}_T$, can represent the best similar level between these two data samples in the time domain, as follows.

$$\hat{\tau} = \arg\max_{\tau} \hat{R}_{12}(\tau) , \tag{8}$$

$$\hat{R}_T = \hat{R}_{12}(\hat{\tau}) . \tag{9}$$

2.3 Similarity evaluation

Based on the normalized deviation degree and the best normalized cross-correlation coefficient constructed in Section 2.2, the similar level (*SL*) between the two data sample sets can be evaluated. In general, the deviation degree $\hat{D}_A$ has a negative correlation with the similarity, but the cross-correlation coefficient $\hat{R}_T$ has a positive correlation with it. Then, the similar level (*SL*) between two data sample sets can be evaluated by their average difference, as shown in Eq. (10),

$$SL_{dif} = \frac{1}{k}\sum_{i=1}^{k} \hat{R}_{Ti} - \frac{1}{k}\sum_{i=1}^{k} \hat{D}_{Ai} , \tag{10}$$

where $\hat{R}_{Ti}$ and $\hat{D}_{Ai}$ are the normalized deviation degree and the best normalized cross-correlation coefficient based on the data sample of sensor i, and k is the number of sensors whose data samples are used to evaluate the similarity.

Furthermore, because both the normalized deviation degree and the best normalized cross-correlation coefficient locate in [0,1], the Euclidean distance between points ($\hat{R}_{Ti}$, $\hat{D}_{Ai}$) and (0, 1) can also be used to measure the similarity of the two data samples. Therefore, the average distance between points ($\hat{R}_{Ti}$, $\hat{D}_{Ai}$) and (0, 1) can be used as another similar level index, as shown in Eq.(11) ,

$$SL_{dis} = \frac{1}{\sqrt{2}k}\sum_{i=1}^{k} \sqrt{\left(\hat{R}_{Ti}-0\right)^2 + \left(\hat{D}_{Ai}-1\right)^2} . \tag{11}$$

2.4 Identification method

For a piece of machine tool operation under an unknown working condition, the monitored sensor data samples measured by k sensors at time t are denoted as

$$\boldsymbol{D}(t) = [\boldsymbol{d}_1(t), \boldsymbol{d}_2(t), ..., \boldsymbol{d}_k(t)] . \tag{12}$$

The benchmark data samples for each sensor are denoted as $\boldsymbol{d}_{0ij}$, where i=1, 2, 3, …, N_j, and j=1, 2, 3, ..., k. N_j is the number of benchmark data samples at different moments for sensor j. The identification method for this unknown working condition can be finished by the following framework.

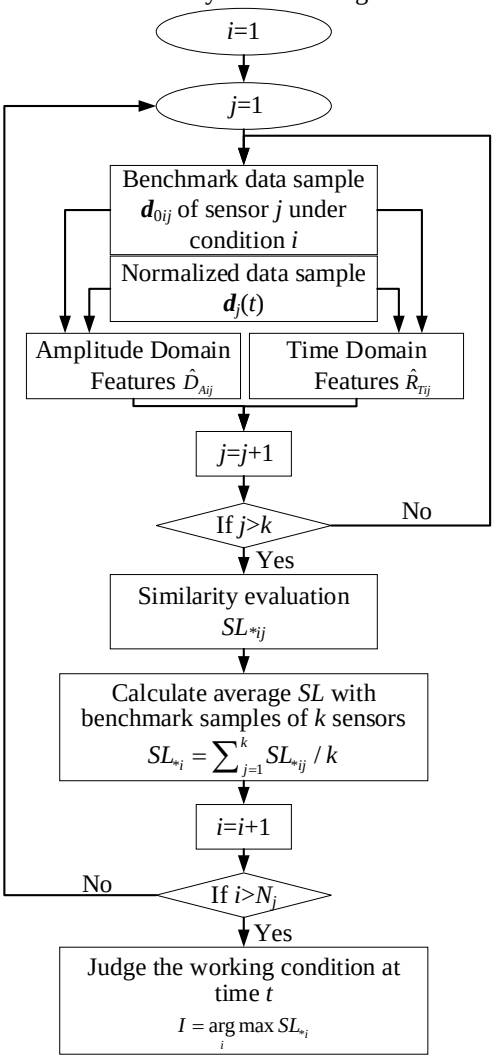

Fig. 3 SL-based identification method framework

2.5 Optimal sensor combination

As stated in Section 2.1, there is a total of n sensors used to monitor the status of concerned objects. However, no data samples from all sensors are sensitive to working conditions. Therefore, a sensitivity analysis of sensor data for working conditions should be done to select optimal sensor fusion. For an n-sensor monitoring system, the number of possible sensor-fusion types can be calculated by,

$$Num = C_n^1 + C_n^2 + ... + C_n^k + ... + C_n^n, \quad (13)$$

where C_n^k is the number of combinations when selecting k objects from n objects. To obtain the optimal sensor-fusion combination, a sensor-data set with known condition types is required to evaluate their accuracy rates of similarity evaluation. Denote the accuracy rate of the ith sensor combination is r_{ai}, then the optimal sensor-fusion type for working condition identification can be illustrated as

$$Y = \arg\max_y \{r_{a1}, r_{a2}, ,...r_{ay}, ..., r_{aNum}\}, \quad (14)$$

where Y is the serial number of optimal combinations, and $Y \in \{1, 2, 3, \ldots, Num\}$. And Fig. 4 provides the detailed method for the evaluation of optimal sensor combination.

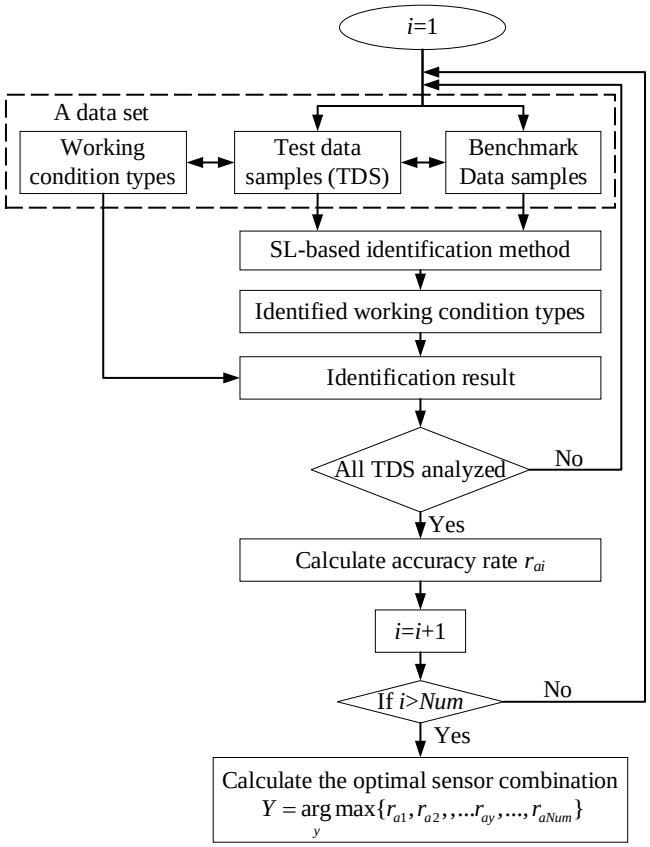

Fig. 4 Evaluating method of optimal sensor combination

2.6 A comparison method

To evaluate the performance of the proposed methods, 11 time-domain features and 13 frequency-domain features proposed in Reference [18] are used as contrast ones. The corresponding time-domain features and frequency-domain features are listed in Tables 1 and 2, respectively.

Table 1 Time-domain features

$F_1 = \frac{1}{l}\sum_{i=1}^{l} d(i)$	$F_7 = \frac{\sum_{i=1}^{l}(d(i)-F_1)^4}{(l-1)F_2^4}$
$F_2 = \sqrt{\frac{\sum_{i=1}^{l}(d(i)-F_1)^2}{l-1}}$	$F_8 = \frac{F_5}{F_4}$
$F_3 = \left(\frac{1}{l}\sum_{i=1}^{l}\sqrt{\lvert d(i)\rvert}\right)^2$	$F_9 = \frac{F_5}{F_3}$
$F_4 = \sqrt{\frac{1}{l}\sum_{i=1}^{l}(d(i))^2}$	$F_{10} = \frac{F_4}{\frac{1}{l}\sum_{i=1}^{l}\lvert d(i)\rvert}$
$F_5 = \max\lvert d(i)\rvert$	$F_{11} = \frac{F_5}{\frac{1}{l}\sum_{i=1}^{l}\lvert d(i)\rvert}$
$F_6 = \frac{\sum_{i=1}^{l}(d(i)-F_1)^3}{(l-1)F_2^3}$	

where $d(i)$ is a signal series of sample value for i=1, 2, …, l.

Table 2 Frequency-domain features

$F_{12} = \frac{1}{m}\sum_{i=1}^{m} s(i)$	$F_{19} = \sqrt{\frac{\sum_{i=1}^{m} f_i^4 s(i)}{\sum_{i=1}^{m} f_i^2 s(i)}}$
$F_{13} = \frac{1}{m-1}\sum_{i=1}^{m}(s(i)-F_{12})^2$	$F_{20} = \frac{\sum_{i=1}^{m} f_i^2 s(i)}{\sqrt{\sum_{i=1}^{m} s(i)\sum_{i=1}^{m} f_i^4 s(i)}}$
$F_{14} = \frac{\sum_{i=1}^{m}(s(i)-F_{12})^3}{m\left(\sqrt{F_{13}}\right)^3}$	$F_{21} = \frac{F_{17}}{F_{16}}$
$F_{15} = \frac{\sum_{i=1}^{m}(s(i)-F_{12})^4}{mF_{13}^2}$	$F_{22} = \frac{\sum_{i=1}^{m}(f_i-F_{16})^3 s(i)}{mF_{17}^3}$
$F_{16} = \frac{\sum_{i=1}^{m} f_i s(i)}{\sum_{i=1}^{m} s(i)}$	$F_{23} = \frac{\sum_{i=1}^{m}(f_i-F_{16})^4 s(i)}{mF_{17}^4}$
$F_{17} = \sqrt{\frac{1}{m}\sum_{i=1}^{m}(f_i-F_{16})^2 s(i)}$	$F_{24} = \frac{\sum_{i=1}^{m}(f_i-F_{16})^{1/2} s(i)}{m\sqrt{F_{17}}}$
$F_{18} = \sqrt{\frac{\sum_{i=1}^{m} f_i^2 s(i)}{\sum_{i=1}^{m} s(i)}}$	

where $s(i)$ is a spectrum for i=1, 2, 3, …, m; m is the number of spectrum lines; f_i is the frequency value of the ith spectrum line.

For a given data sample set from different sensors and a monitoring system with n sensors, there will be a total of n×24 sensor and feature combinations for identification. First, a sensitive evaluation is done to find the best sensor and feature combination $\boldsymbol{F}_{opt}=[F_a, F_b, \ldots,]$ based on the feature evaluation method in Reference [19]. Then, corresponding working condition identifications are implemented based on the optimal sensor and feature combination. For any working

condition with sensor data sample $\boldsymbol{d}$, the feature difference DF_i between it and any benchmark data sample $\boldsymbol{b}_i$ can be calculated by

$$DF_i = \left| \boldsymbol{F}_{opt}(\boldsymbol{d}) - \boldsymbol{F}_{opt}(\boldsymbol{b}_i) \right|, \quad (15)$$

and then the working condition whose benchmark data sample has the lowest feature difference with sensor data sample $\boldsymbol{d}$ is judged as it working condition, as follows,

The flowchart of the used comparison method is shown in Fig. 5.

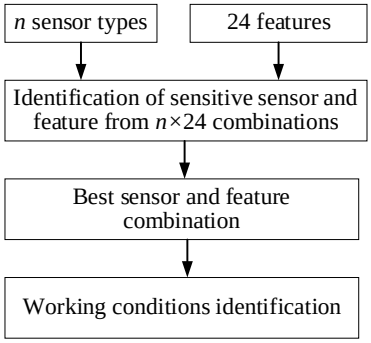

Fig. 5 Flowchart of working condition identification

3. Case Study

3.1 A data set

NASA Ames prognostics data repository is a growing source covering several sets of prognostic data contributed by universities, companies, or agencies [20], [21], which provides a dataset of flank wear on the milling insert under different working conditions [22]. In detail, the Matsuura machining canter MC-510V was used to generate the degradation dataset, where the size of processed workpieces was 483mm×178mm×51mm. Also, materials (cast iron and stainless steel J45), DOC (1.50mm and 0.75mm), and Feed (0.5mm/rev and 0.25mm/rev) are used as working condition variables (Material, DOC, and Feed,). Therefore, total n_h=2^3=8 working conditions were studied in the experiment as shown in Table 1. n=6 sensors were used to measure AC and DC spindle motor current, table and spindle vibration, and acoustic emission at the table and spindle, respectively. A total of 16 cases including 165 groups of valid degradation and sensor data were given.

Table 3 Homogeneous conditions studied in the experiments

Condition 1: Cast Iron/1.50/ 0.50;
Condition 2: Cast Iron/1.50/ 0.25;
Condition 3: Cast Iron/0.75/ 0.50;
Condition 4: Cast Iron/0.75/ 0.25;
Condition 5: Steel/1.50/ 0.50;
Condition 6: Steel/1.50/ 0.25;
Condition 7: Steel/0.75/ 0.50;
Condition 8: Steel/0.75/ 0.25.

Based on the proposed identification methods, the case studies different identification experiments for working conditions under different situations. Three situation variables are considered, as shown in Table 4. Then, a structure of 'Data type - Amplitude type - Similarity index' is used to illustrate different experiment situations. For example, 'OYS' means the similarity is evaluated by the 'average distance'-based SL_{dis} and the sensor data is the 'original full data in four stages' with 'normalized amplitudes'. Therefore, there will be a total of 2^3=8 experiment situations for the proposed method.

Table 4 Experiment situations

Variables	Descriptions	Symbols
Data types	Original full data in four stages	O
	Partial data in steadily cutting stage	S
Amplitude types	Normalized amplitudes	Y
	Original amplitudes	N
Similarity indexes	Average difference	F
	Average distance	S

Further, for the comparison method, the features are used as the similarity index. Therefore, the experiment situation is illustrated by a structure of 'Data type - Amplitude type'. For example, 'SY' means the similarity is evaluated by the feature of sensor data which is the 'partial data in steadily cutting stage' with 'normalized amplitudes'. Therefore, there will be a total of 2^2=4 experiment situations for the comparison method.

3.2 Identification analysis

Based on the evaluation method for optimal sensor combinations proposed in Section 2.5, different experiments are implemented to identify combined working conditions shown in Table 3 or individual working-condition variables (DOC, Feed, Material). The corresponding accuracy rates under different methods and situations are illustrated in Table 5.

Table 5 Accuracy rates under different methods and situations

Methods	Situations	Condition variables			Combined conditions
		DOC	Feed	Material	
Proposed method	OYF	0.812	0.921	0.921	0.503
	OYS	0.800	0.945	0.921	0.673
	ONF	0.715	0.982	0.600	0.279
	ONS	0.782	0.994	0.673	0.297
	SYF	0.739	0.648	0.752	0.291
	SYS	0.733	0.655	0.752	0.261
	SNF	0.691	0.655	0.545	0.364
	SNS	0.897	0.915	0.770	0.364
Comparison method	OY	0.703	0.988	0.642	0.388
	ON	0.727	0.939	0.830	0.388
	SY	0.758	0.624	0.818	0.309
	SN	0.624	0.588	0.848	0.309

The identification performance for combined conditions under the proposed and comparison methods is illustrated in Fig. 6. In general, both the proposed and comparison methods show a low accuracy rate for the combined condition identification. In the best cases, the proposed method could obtain a better accuracy rate of 0.673 under the 'OYS' situation that the similarity is evaluated by the 'average distance'-based SL_{dis} and the sensor data is the 'original full

data in four stages' with 'normalized amplitudes'. Besides, both the situations 'OYF', 'OYS', and 'OY' could help the corresponding method obtain a relatively higher accuracy rate than other situations. Therefore, the applications of original full data in four stages and normalized amplitudes could help improve the identification performance.

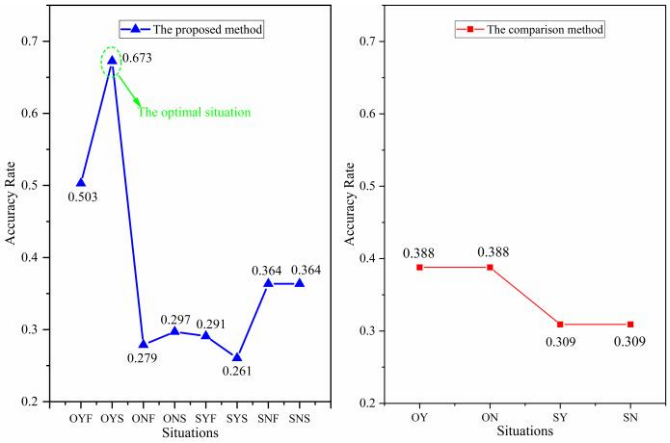

Fig. 6 Accuracy rates for combined condition identifications

Besides, for the identification of condition variables under the proposed method, the best accuracy rates are 0.897, 0.994, and 0.921 for DOC, Feed, and material, which are obtained under the situations 'SNS', 'ONS', and 'OYF' (or 'OYS'), respectively, as shown in Table 5. By the comparison method, the corresponding best accuracy rates are 0.758, 0.988, and 0.848, which are obtained under the situations 'SY', 'OY', and 'SN', respectively. The proposed method can also obtain a better accuracy rate than the comparison method for the identification of individual working-condition variables.

Also, through controlling the change of condition variables, the comparison histograms of accuracy rates for different condition variables by the proposed method are given in Fig. 7. Fig. 7(a) represents that the change of data types brings a coincident changing direction for the accuracy rates of DOC, Feed, and Material. In detail, when situation 'OYF' switches to 'SYF', meaning that original full data in four stages is replaced by the partial data in the steadily cutting stage, all the accuracy rates of DOC, Feed, and Material will decrease, as shown in Fig. 7(a). The situation variable bringing a coincident change in accuracy rates of all condition variables is defined as the strong situation variable.

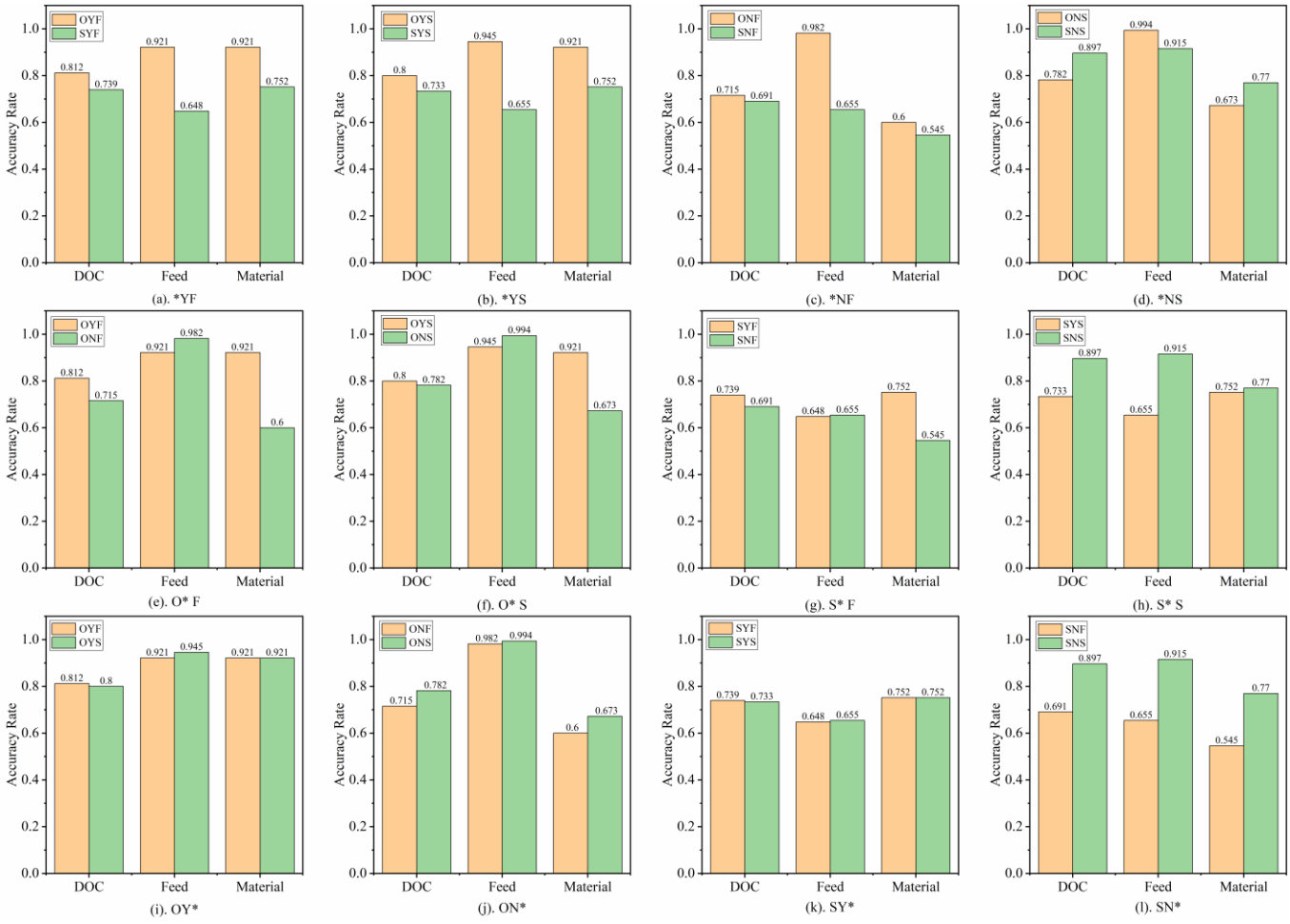

Fig. 7 Histogram comparison of accuracy rates for condition variable identification by the proposed method

As shown in Fig. 7(a)~(d), the situation variables amplitude type and similarity index are controlled, and data type changes (O or S) in each histogram. The accuracy rates of DOC, Feed, and Material have a coincident change when data type changes in Fig. 7(a), (b), and (c). In Fig. 7(e)~(h), the situation variables data type and similarity index are controlled, and the amplitude type changes (Y or N). And the accuracy rates of DOC, Feed, and Material have a coincident change when amplitude type changes only in Fig. 7(h). In Fig. 7(i)~(l), the situation variables data type and amplitude type are controlled, but the similarity index changes (F or S). And the accuracy rates of DOC, Feed, and Material have a coincident change when the similarity index changes in Fig. 7(j) and (l). According to the frequency being a strong situation variable in histograms, it can be concluded that the influence intensity of situation variables to accuracy rate has the following relationships,

$$\text{Data type} > \text{Similarity index} > \text{Amplitude type}. \quad (16)$$

4. Conclusion

Various monitored sensor signals provide rich data for the RUL predictions, where the identification of heterogeneous working conditions is necessary. To provide an effective method for the identification of current working conditions and state transition trajectories of future working conditions, this article proposed a similarity evaluation method based on the constructed amplitude-domain and time-domain features. Also, a similarity evaluation framework and a flowchart for selecting the optimal sensor combination are proposed. Then, a case study based on a degradation dataset of milling insert proves the effectiveness of our proposed method.

The result implies that identification performance for combined conditions is inferior to the one for individual working-condition variables. Also, it proves that the applications of original full data in four stages and normalized amplitudes could help improve the identification performance. And completeness level of sensor data in all stages has a strong relationship with the accuracy rate of identifications. In the future, based on the proposed method, an adaptive RUL prediction can be explored to dynamically prognosticate the status of a machine tool under heterogeneous working conditions. Also, this article only provides a traditional feature-based similarity evaluation. However, artificial intelligence provides a much brighter prospect for condition identification. In the future, AI-based working-condition identification and adaptive RUL prediction should be further studied.

5. Acknowledgements

This work was supported by the National Natural Science Foundation of China [72201250, 72271200].

6. References

[1] C. Shi, G. Panoutsos, B. Luo *et al.*, "Using Multiple-Feature-Spaces-Based Deep Learning for Tool Condition Monitoring in Ultraprecision Manufacturing," *IEEE Transactions on Industrial Electronics*, vol. 66, no. 5, pp. 3794-3803. 2019.

[2] M. Pratama, E. Dimla, T. Tjahjowidodo *et al.*, "Online Tool Condition Monitoring Based on Parsimonious Ensemble+," *IEEE Transactions on Cybernetics*, vol. 50, no. 2, pp. 664-677. 2020.

[3] Z. You, H. Gao, S. Li *et al.*, "Multiple Activation Functions and Data Augmentation-Based Lightweight Network for In Situ Tool Condition Monitoring," *IEEE Transactions on Industrial Electronics*, vol. 69, no. 12, pp. 13656-13664. 2022.

[4] Z. Ye, H. Yang, Z. Cai *et al.*, "Performance evaluation of serial-parallel manufacturing systems based on the impact of heterogeneous feedstocks on machine degradation," *Reliability Engineering & System Safety*, vol. 207, pp. 107319, Mar. 2021.

[5] Z. Ye, S. Si, H. Yang *et al.*, "Machine and Feedstock Interdependence Modeling for Manufacturing Networks Performance Analysis," *IEEE Transactions on Industrial Informatics*, vol. 18, no. 8, pp. 5067-5076, Aug. 2022.

[6] Z. Ye, Z. Cai, S. Si *et al.*, "Operational reliability and quality loss of diversely configurated manufacturing cells with heterogeneous feedstocks," *Proceedings of the Institution of Mechanical Engineers, Part O: Journal of Risk and Reliability*, vol. 236, no. 6, pp. 955-967. 2022.

[7] Z. Zhang, X. Si, C. Hu *et al.*, "Degradation modeling–based remaining useful life estimation: A review on approaches for systems with heterogeneity," *Proceedings of the Institution of Mechanical Engineers, Part O: Journal of Risk and Reliability*, vol. 229, no. 4, pp. 343-355, Aug. 2015.

[8] K. Lin, Y. Chen, and D. Xu, "Reliability assessment model considering heterogeneous population in a multiple stresses accelerated test," *Reliability Engineering & System Safety*, vol. 165, pp. 134-143, Sep. 2017.

[9] J. H. Cha, and M. Finkelstein, "The failure rate dynamics in heterogeneous populations," *Reliability Engineering & System Safety*, vol. 112, pp. 120-128, Apr. 2013.

[10] Y. Cheng, Y. Wei, and H. Liao, "Optimal sampling-based sequential inspection and maintenance plans for a heterogeneous product with competing failure modes," *Reliability Engineering & System Safety*, vol. 218, pp. 108181, Feb. 2022.

[11] G. A. Veloso, and R. H. Loschi, "Dynamic linear degradation model: Dealing with heterogeneity in degradation paths," *Reliability Engineering & System Safety*, vol. 210, pp. 107446, Jun. 2021.

[12]B. Lu, Z. Chen, and X. Zhao, “Data-driven dynamic adaptive replacement policy for units subject to heterogeneous degradation,” *Computers & Industrial Engineering*, pp. 108478, Jul. 2022.

[13]A. Moniri-Morad, M. Pourgol-Mohammad, H. Aghababaei *et al.*, “Reliability-based covariate analysis for complex systems in heterogeneous environment: Case study of mining equipment,” *Proceedings of the Institution of Mechanical Engineers, Part O: Journal of Risk and Reliability*, vol. 233, no. 4, pp. 593-604, Sep. 2018.

[14]R. Barabadi, M. Ataei, R. Khalokakaie *et al.*, “Spare-part management in a heterogeneous environment,” *PLOS ONE*, vol. 16, no. 3, pp. e0247650. 2021.

[15]Z. Allahkarami, A. R. Sayadi, and B. Ghodrati, “Mixed-effects model for reliability assessment of dump trucks in heterogeneous operating environment: A case study,” *Quality and Reliability Engineering International*, vol. In press, pp. 1-18. 2022.

[16]X. Si, “An Adaptive Prognostic Approach via Nonlinear Degradation Modeling: Application to Battery Data,” *IEEE Transactions on Industrial Electronics*, vol. 62, no. 8, pp. 5082-5096. 2015.

[17]S. Xing, Y. Lei, B. Yang *et al.*, “Adaptive Knowledge Transfer by Continual Weighted Updating of Filter Kernels for Few-Shot Fault Diagnosis of Machines,” *IEEE Transactions on Industrial Electronics*, vol. 69, no. 2, pp. 1968-1976. 2022.

[18]Y. Lei, Z. He, Y. Zi *et al.*, “Fault diagnosis of rotating machinery based on multiple ANFIS combination with GAs,” *Mechanical Systems and Signal Processing*, vol. 21, no. 5, pp. 2280-2294, Jul. 2007.

[19]X. Chen, and Y. Zi, *Intelligent maintenance and health management*, 1 ed.: China machine press, 2020.

[20]O. F. Eker, F. Camci, and I. K. Jennions, "Major challenges in prognostics: Study on benchmarking prognostics datasets." PHM Society European Conference, 2012.

[21]Y. Lei, N. Li, L. Guo *et al.*, “Machinery health prognostics: A systematic review from data acquisition to RUL prediction,” *Mechanical Systems and Signal Processing*, vol. 104, pp. 799-834, May. 2018.

[22]A. Agogino, and K. Goebel, "Milling Data Set," U. B. BEST lab, ed., 2007.